Spin Evolution and Decoherence

Richard Talman
Laboratory for Elementary-Particle Physics
Cornell University

September 24, 2017

Abstract

Miscellaneous spin evolution topics are discussed, including spin decoherence and the futility of applying Siberian snakes to EDM measurement in magnetic storage rings.

Contents

1 Spin evolution

1.1 Spin and bend coordinates

For studying spin evolution in a frozen spin storage ring we use the coordinate system shown in Figure 1. The instantaneous local frame of reference is the Frenet frame aligned with the orbit of an individual particle being tracked, with $\mathbf{e_1}$ pointing in the centrifugal (outward) direction, $\mathbf{e_3}$ pointing in the tangential direction and $\mathbf{e_2}$ pointing up, out of the plain. The figure shows the angle $\tilde{\alpha}$ which is the angle in the instantaneous bend plane between the projection of the spin vector onto the bend plane and $\mathbf{e_3}$, which is tangent to the particle orbit.

Globally, spin precession is most naturally described by using, as spin coordinates, s_y, the vertical component of spin in the laboratory frame, and α, the angle between the component of the projection of the spin vector onto the (horizontal) design frame and the local design orbit. The purpose for the overhead tilde $\tilde{\alpha}$ (and all subsequent overhead tildes) is to indicate that this projection is being taken in the instantaneous orbit plane, which is very nearly, though not exactly, the same as the ideal horizontal plane. In these notes this distinction will mainly be ignored, since the effects are expected to be negligible in an ultraweak focusing proton EDM lattice.

Though the spin vector has three components, only two are independent; the angle $\tilde{\alpha}$ fixes the direction of $\tilde{\mathbf{s}}_\parallel$ in the bend plane. The spin precesses about the $\tilde{y}$-axis in the bend plane. The bend frame spin coordinates are

$$\begin{pmatrix} \tilde{s}_x \\ \tilde{s}_y \\ \tilde{s}_z \end{pmatrix} = \begin{pmatrix} -\tilde{s}_\parallel \sin\tilde{\alpha} \\ \tilde{s}_\perp \\ \tilde{s}_\parallel \cos\tilde{\alpha} \end{pmatrix}. \tag{1}$$

Two parameters are sufficient because the magnitude of $\tilde{\mathbf{s}}$ is equal to 1;

$$\tilde{s}_\parallel^2 + \tilde{s}_\perp^2 = 1. \tag{2}$$

(Note that $\tilde{\mathbf{s}}_\parallel$ is the 2D vector component of the spin vector in the bend plane, *not* the component of the spin vector parallel to the velocity.) These coordinates are ideal for evolving the spins through the (dominant) ring horizontal bending elements.

1.1.1 Transformation between design frame and bend frame

From particle tracking one knows the laboratory frame vectors $\mathbf{r}$, $\mathbf{p}$, and hence $\mathbf{L} = \mathbf{r} \times \mathbf{p}$, and one also has the spin vector $\mathbf{s}$;

$$\begin{aligned} \mathbf{r} &= r_x\hat{\mathbf{x}} + r_y\hat{\mathbf{y}} + r_z\hat{\mathbf{z}}, \\ \mathbf{p} &= p_x\hat{\mathbf{x}} + p_y\hat{\mathbf{y}} + p_z\hat{\mathbf{z}}, \\ \mathbf{L} &= L_x\hat{\mathbf{x}} + L_y\hat{\mathbf{y}} + L_z\hat{\mathbf{z}}, \\ \mathbf{s} &= s_x\hat{\mathbf{x}} + s_y\hat{\mathbf{y}} + s_z\hat{\mathbf{z}}. \end{aligned} \tag{3}$$

Initially, for example, these quantities refer to a point just past the entrance of a bending element. Any spin precession in the interior of a bend element occurs in the bend plane. To

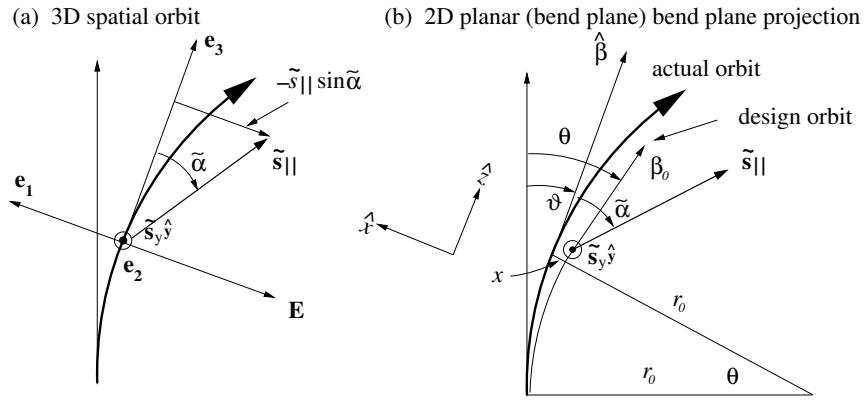

Figure 1: (a) In the bend plane the spin vector $\mathbf{s}$ has precessed through angle $\tilde{\alpha}$ away from its nominal direction along the proton's velocity. (Different particles have different bend planes, but the this distinction is being neglected.) (b) Projection of figure (a) onto the laboratory horizontal plane. The projected longitudinal axis is shown coinciding with the laboratory longitudinal axis, even if this is not exactly valid. x is the deviation of the (bold face) particle orbit from the (pale face) design orbit. If the bend plane coincides with the design bend plane (as is always approximately the case) $\hat{\boldsymbol{\beta}}_0$ and $\hat{\mathbf{z}}$ are identical. θ is the reference particle global horizontal angle and ϑ is the tracked particle global horizontal angle. On the average θ and ϑ are the same, but betatron oscillations cause them to differ on a turn by turn basis, and also to make the instantaneous bend plane not quite horizontal.

exploit this reduction from 3D to 2D it is first necessary to obtain the spin components in an orthonormal frame having its "y" axis perpendicular to the plane and its "z" coordinate tangential to the orbit. The purpose of this section is to document this transformation. In the (always excellent) paraxial approximation, this transformation will be close to identity.

We can establish an orthonormal, right-handed basis triad with axis 3 parallel to $\mathbf{p}$ and axis 2 parallel to $-\mathbf{L}$ (where the negative sign is appropriate for clockwise orbits);

$$\begin{aligned}
\mathbf{e_3} &= \frac{p_x}{p}\,\hat{\mathbf{x}} + \frac{p_y}{p}\,\hat{\mathbf{y}} + \frac{p_z}{p}\,\hat{\mathbf{z}}, \\
\mathbf{e_2} &= \frac{\mathbf{r}\times\mathbf{p}}{-L}, \\
\mathbf{e_1} &= \mathbf{e_2}\times\mathbf{e_3}.
\end{aligned} \tag{4}$$

These equations can be re-expressed formally, with all coefficients known, as

$$\begin{aligned}
\mathbf{e_1} &= a_{11}\hat{\mathbf{x}} + a_{12}\hat{\mathbf{y}} + a_{13}\hat{\mathbf{z}} \\
\mathbf{e_2} &= a_{21}\hat{\mathbf{x}} + a_{22}\hat{\mathbf{y}} + a_{23}\hat{\mathbf{z}} \\
\mathbf{e_3} &= a_{31}\hat{\mathbf{x}} + a_{32}\hat{\mathbf{y}} + a_{33}\hat{\mathbf{z}}.
\end{aligned} \tag{5}$$

The vector $\mathbf{s}$ can be expanded as

$$\begin{aligned}\mathbf{s} &= \tilde{s}_1\mathbf{e_1} + \tilde{s}_2\mathbf{e_2} + \tilde{s}_3\mathbf{e_3} \\ &= \tilde{s}_1(a_{11}\hat{\mathbf{x}} + a_{12}\hat{\mathbf{y}} + a_{13}\hat{\mathbf{z}}) + \dots \\ &= (a_{11}\tilde{s}_1 + a_{21}\tilde{s}_2 + a_{31}\tilde{s}_3)\,\hat{\mathbf{x}} + \dots . \end{aligned} \tag{6}$$

The final relation can be expressed in matrix form as

$$\begin{pmatrix} s_x \\ s_y \\ s_z \end{pmatrix} = \mathbf{R} \begin{pmatrix} \tilde{s}_1 \\ \tilde{s}_2 \\ \tilde{s}_3 \end{pmatrix}, \tag{7}$$

where $\mathbf{R}$ is an orthogonal matrix,

$$\mathbf{R} = \begin{pmatrix} a_{11} & a_{21} & a_{31} \\ a_{12} & a_{22} & a_{32} \\ a_{13} & a_{23} & a_{33} \end{pmatrix}. \tag{8}$$

(Aside: the magnitude $|\det\mathbf{R}|$ of the determinant of $\mathbf{R}$ is necessarily 1, but the actual value is ± 1. This sign correlates with the clockwise/counterclockwise orbit ambiguity.)

Because $\mathbf{R}$ is orthogonal, $\mathbf{R}^{-1} = \mathbf{R}^T$ and Eq. (7) can be inverted to give

$$\begin{pmatrix} \tilde{s}_1 \\ \tilde{s}_2 \\ \tilde{s}_3 \end{pmatrix} = \begin{pmatrix} a_{11} & a_{12} & a_{13} \\ a_{21} & a_{22} & a_{23} \\ a_{31} & a_{32} & a_{33} \end{pmatrix} \begin{pmatrix} s_x \\ s_y \\ s_z \end{pmatrix}. \tag{9}$$

This yields the spin components in the bend frame. Their propagation through the bend is described below.

After the bend plane spin components have been updated at the output of a bend element it is necessary to transform them back to the (local) laboratory frame. This entails repeating the preceeding formulas starting with Eqs (3), but with $\mathbf{r}$, $\mathbf{p}$ and $\mathbf{L}$ having been evaluated (in local laboratory coordinates) just inside the output face of the bend element. In other words, all of the quantities in Eqs. (3) now refer to a point just before the bend exit. Then, the following Eqs. (4) through (8) produce rotation matrix $\mathbf{R}$ which is now applicable at the bend output. Finally, modifying Eq. (9) appropriately, the transformation back to laboratory components is

$$\begin{pmatrix} s_x \\ s_y \\ s_z \end{pmatrix} = \begin{pmatrix} a_{11} & a_{12} & a_{13} \\ a_{21} & a_{22} & a_{23} \\ a_{31} & a_{32} & a_{33} \end{pmatrix}^T \begin{pmatrix} \tilde{s}_1 \\ \tilde{s}_2 \\ \tilde{s}_3 \end{pmatrix}. \tag{10}$$

1.2 Spin evolution through bends

For motion restricted to a single plane (which is implicit in the present discussion) the BMT equation can be solved exactly in closed form. In this frame any precession of the spin is purely around an axis normal to the plane. For the 2D evolution through electric bend elements, vertical betatron oscillations are neglected. Any betatron oscillations actually present are treated as exactly horizontal.

As shown in Figure 1, the initial spin vector is

$$\tilde{\mathbf{s}} = -\tilde{s}_{\|} \sin\tilde{\alpha}\,\hat{\mathbf{x}} + \tilde{s}_y\hat{\mathbf{y}} + \tilde{s}_{\|}\cos\tilde{\alpha}\,\hat{\mathbf{z}}. \tag{11}$$

Here $\tilde{s}_y\hat{\mathbf{y}}$ is the out-of-plane component of $\tilde{\mathbf{s}}$, $\tilde{s}_{\|}$ is the magnitude of the in-plane projection of $\tilde{\mathbf{s}}$, and $\tilde{\alpha}$ is the angle between the projection of $\tilde{\mathbf{s}}$ onto the plane and the tangent vector to the orbit.

Jackson's[1] Eq. (11.171) gives the rate of change in an electric field $\mathbf{E}$, of the longitudinal spin component as

$$\frac{d}{dt}\,(\hat{\beta}\cdot\mathbf{s}) = -\frac{e}{m_p c}\,(\mathbf{s}_{\perp,\mathbf{J}}\cdot\mathbf{E})\left(\frac{g\beta}{2}-\frac{1}{\beta}\right). \tag{12}$$

(Note that Jackson's $\mathbf{s}_{\perp,J}$ is the component perpendicular to the tangent to the orbit *not* to the orbit plane.) Substituting from Eq. (11) the equation becomes

$$\frac{d}{dt}\,(\tilde{s}_{\|}\cos\tilde{\alpha}) = -\frac{e}{m_p c}\,(\tilde{s}_{\|}\sin\tilde{\alpha}\,E)\left(\frac{g\beta}{2}-\frac{1}{\beta}\right). \tag{13}$$

With the orbit confined to a plane, any precession occurs about the normal to the plane, conserving $\tilde{s}_y$. Since the magnitude of $\tilde{\mathbf{s}}$ is conserved it follows that the magnitude $\tilde{s}_{\|}$ is also conserved. This allows $\tilde{s}_{\|}$ to be treated as constant in Eq. (13). Then Eq. (13) reduces to

$$\frac{d\tilde{\alpha}}{dt} = \frac{eE}{m_p c}\left(\frac{g\beta}{2}-\frac{1}{\beta}\right). \tag{14}$$

This is undoubtedly a fairly good approximate equation in any more-or-less constant electric field, but it is *exact only for motion restricted to a single planr.* In fact, the derivation is not quite valid even for our $m = 1$ case. Though the design orbit is circular, the betatron orbits are slightly elliptic. This violates our assumption that orbit and electric field are orthogonal. Neglecting this amounts to dropping a term from the RHS of Eq. (12) that is down by four orders of magnitude. Furthermore this term would average to zero except for a possible non-zero commutation precession which would be expected to be down by another four orders of magnitude.

Meanwhile the velocity vector itself has precessed by angle ϑ relative to a direction fixed in the laboratory. Note that this angle ϑ, the angle of the individual particle's orbit is approximately, but not exactly equal to the angle θ of the design orbit.

The precession rate of ϑ is governed by the equation

$$\frac{d\vartheta}{dt} = \frac{d}{dt}\left(\frac{s}{r}\right) = \frac{eE}{p}. \tag{15}$$

where the curvature is $1/r = eE/(vp)$ and (just in this equation) s temporarily stands for arc length along the orbit. Dividing Eq. (14) by Eq. (15) and using $pc = m_p c^2\gamma\beta$,

$$\boxed{\frac{d\tilde{\alpha}}{d\theta} = \left(\frac{g}{2}-1\right)\gamma - \frac{g/2}{\gamma}.} \tag{16}$$

In this step we have also surrepticiously made the replacement $\vartheta \to \theta$. Though these angles are not the instantaneously the same, over arbitrarily long times they advance at the same average rate. Explicitly the bend frame precession advance is the sum of two definite integrals

$$\widetilde{\Delta\alpha} = \left(\frac{g}{2} - 1\right) I_\gamma - \frac{g}{2} I_{\gamma i}, \tag{17}$$

where

$$I_\gamma = \int_0^\theta \gamma(\theta') d\theta', \quad \text{and} \quad I_{\gamma i} = \int_0^\theta \frac{d\theta'}{\gamma(\theta')}. \tag{18}$$

To account for fringe fields two more terms, $\widetilde{\Delta\alpha}^{\rm FF,in}$ and $\widetilde{\Delta\alpha}^{\rm FF,out}$, will later be added directly to the right hand side of Eq. (17).

A quicker yet equivalent formula for the precession occuring in a bend element is to use the so-called "spin tune", (derived in an appendix) defined in an electric field by

$$Q_s \equiv \frac{d\alpha}{d\theta}\Big|_E = G\beta^2\gamma - \frac{1}{\gamma} \stackrel{\text{also}}{=} \left(\frac{g}{2} - 1\right)\gamma - \frac{g/2}{\gamma} \tag{19}$$

where α is the angle between spin vector and particle velocity. The bend frame precession advance is then given by

$$\widetilde{\Delta\alpha} = Q_s \Delta\theta, \tag{20}$$

where $\Delta\theta$ is the total magnet bend. The approximation that γ is constant has been used, and the anomalous magnetic moment $G = g/2 - 1$ has been substituted. In our EDM ring, with all orbits having very nearly the magic velocity, every such incremental precession angle is very small.

2 Spin Decoherence

2.1 Virial theorem decoherence determination

In estimating spin decoherence we need to account for the transverse position oscillations accompanying potential energy variation. Initially we analyse the "coasting beam" case in which there is no RF acceleration, or rather no beam bunching, in the ring. For simplicity we also assume, initially, that the lattice is uniform, with no drift regions.

Copying from Eq. (14), the spin precession angle α, relative to the proton direction, evolves as

$$\frac{d\alpha}{dt} = \frac{eE(x)}{m_p c}\left(\frac{g\beta(x)}{2} - \frac{1}{\beta(x)}\right). \tag{21}$$

The variables β, γ, and E in this equation, though permitted to differ from magic values, have been treated as constants of the motion. But we now intend to make allowance for the fact that these dynamic variables depend also on x. We can also improve on Eq. (15) using

$$\frac{d\theta}{dt} = \frac{L}{\gamma m_p r^2}; \tag{22}$$

(which is valid in bend regions, but would not be in drift regions, where r is undefined). In this equation the angular momentum L is a constant of the motion (because the force is radial) but γ and $r = r_0 + x$ depend on x. We combine the two previous equations to obtain

$$\frac{d\alpha}{d\theta} = \frac{eE(x)(r_0+x)^2}{Lc\beta(x)}\left(\Big(\frac{g}{2}-1\Big)\gamma(x) - \frac{g/2}{\gamma(x)}\right), \tag{23}$$

To find the evolution of α over long times we need to average this equation. What makes this averaging difficult is the fact that the final factor has, intentionally, been arranged to cancel for the central, design particle. The initial factor, though not constant, varies over a quite small range. A promising approximation scheme, therefore, in the slowly varying factor on the left, is to neglect the (small) rapidly oscillating contibution to x coming from the betatron oscillation, and retain only the part $x = D_x\gamma^O$ associated with the slowly varying synchrotron oscillation;

$$\left\langle\frac{d\alpha}{d\theta}\right\rangle = \frac{eE(D_x\gamma^O)(r_0+D_x\gamma^O)^2}{Lc\beta(D_x\gamma^O)}\left\langle\Big(\frac{g}{2}-1\Big)\gamma(x) - \frac{g/2}{\gamma(x)}\right\rangle. \tag{24}$$

The remaining $\gamma(x)$ factor is the "inside" gamma factor, but no superscript "I" is needed, since only "inside" motion is under discussion. Note, though, that $\gamma(x)$, as well as varying on a long time scale along with synchrotron oscillation of γ^O, varies on a short time scale due to horizontal betatron oscillations that introduce changes in potential energy. If the average of $\langle\gamma\rangle$ were the inverse of $\langle 1/\gamma\rangle$ the averaging over combined synchrotron and horizontal betatron averaging would be easy, but of course this is not true. However the factorization already applied in Eq. (24) allows the averaging over γ^O to be deferred.

The virial theorem can sometimes be used to obtain average behavior of multiparticle systems subject to central forces. Our application is complicated by the fact that fully relativistic mechanics has to be used. Also, though our electric field is centrally directed within any single deflecting element, because of drift regions in the lattice, the centers of the various deflection elements do not coincide. We can therefore calculate only the spin decoherence applicable to passage through the bend regions, which is where the overwhelmingly dominant part of the momentum evolution occurs. (For completeness we should have (but have not) checked that there is no correlation that could cause these averages to not be strictly additive.)

The independent variables θ and t are very nearly, but not exactly proportional to each other on an instantaneous basis. As a result averages with respect to one or the other are not necessarily instantaneously identical. However, with bunched beams over long times, θ and t are strictly proportional (on the average) and the two forms of averaging have to be essentially identical. Even for unbunched beams we assume the averages are close enough to ignore their difference.

Because there are so many variants of "the virial theorem" it is easier to derive it from scratch than to copy it from one of many possible references. The "virial" G is defined, in terms of radius vector $\mathbf{r}$ and momentum $\mathbf{p}$, by

$$G = \mathbf{r}\cdot\mathbf{p} \tag{25}$$

Our electric field is

$$\mathbf{E} = -E_0\Big(\frac{r_0}{r}\Big)^{1+m}\widehat{\mathbf{r}}, \tag{26}$$

and Newton's law gives

$$\frac{d\mathbf{p}}{dt} \equiv m_p \frac{d}{dt}(\gamma \mathbf{v}) = e\mathbf{E}. \tag{27}$$

In a bending element the time rate of change of $\mathbf{G}$ is given by

$$\begin{aligned} \left.\frac{dG}{dt}\right|_{\text{bend}} &= \dot{\mathbf{r}} \cdot \mathbf{p} + \mathbf{r} \cdot \dot{\mathbf{p}} \\ &= m_p \gamma v^2 - eE_0 \frac{r_0^{1+m}}{r^m} \\ &= m_p c^2 \gamma - m_p c^2 \frac{1}{\gamma} - eE_0 r_0 \frac{r_0^m}{r^m}. \end{aligned} \tag{28}$$

Averaging over time, presuming bounded motion, and therefore requiring $\langle dG/dt \rangle$ to vanish, one obtains

$$\left\langle \frac{1}{\gamma} \right\rangle = \langle \gamma \rangle - \frac{E_0 r_0}{m_p c^2/e} \left\langle \frac{r_0^m}{r^m} \right\rangle. \tag{29}$$

This provides the needed relation between $\langle \gamma \rangle$ and $\langle 1/\gamma \rangle$. Applying this result to (time)-average Eq. (24) yields

$$\left\langle \frac{d\alpha}{d\theta} \right\rangle = \frac{eE(D_x\gamma^O)(r_0 + D_x\gamma^O)^2}{Lc\beta(D_x\gamma^O)} \left(-\langle \gamma \rangle + \frac{g}{2} \frac{E_0 r_0}{m_p c^2/e} \left\langle \frac{r_0^m}{r^m} \right\rangle \right). \tag{30}$$

For simplifying this result the following formulas can be employed:

$$\begin{aligned} \gamma(x) &\equiv \gamma_0 + \Delta\gamma, \\ \frac{E_0 r_0}{m_p c^2/e} &= \gamma_0 - \frac{1}{\gamma_0}, \\ \frac{r_0^m}{r^m} &\approx 1 - m\frac{x}{r_0}, \\ \gamma_0 &= \frac{g}{2}\left(\gamma_0 - \frac{1}{\gamma_0}\right). \end{aligned} \tag{31}$$

As written, these formulas assume the beam centroid energy and the storage ring lattice are exactly matched at the frozen spin magic value. To the extent this is not true the spin orientation would change monitonically. What is being calculated is the spin orientation spreading relative to the mean orientation.

For perfectly sinusoidal synchrotron oscilations, which we assume initially, the initial factor can be replaced by its average value. This yields

$$\left\langle \frac{d\alpha}{d\theta} \right\rangle \approx -\frac{eE_0 r_0^2}{Lc\beta_0} \left(\langle \Delta\gamma^I \rangle + \frac{g}{2} \frac{m}{r_0} \left(\gamma_0 - \frac{1}{\gamma_0}\right) \langle x \rangle \right). \tag{32}$$

(The superscript "I" has been restored as a reminder that $\Delta\gamma^I$ is evaluated within bend elements, as contrasted to within drift sections.)

For $m = 0$ both terms in Eq. (32) vanish. Although it is not obvious from the notation, the term $\langle \Delta\gamma^I \rangle$ on the right hand side of the equation depends on m. In fact, we know

that for $m \approx 0$, in a weak-focusing lattice, $\Delta\gamma^I$ becomes very small. Furthermore, for our proposed WW-AG-CF lattice, even this weak decoherence is cancelled to lowest order by the alternating m-value, even without the benefit of synchrotron oscillation averaging.

We have shown, therefore, for the WW-AG-CF lattice, that decoherence in the bend regions can be neglected even in the presence of horizontal betatron oscillations, We have previosly argued (though perhaps not persuasively enough) that decoherence associated with vertical betatron oscillation can also be neglected.

Numerical simulation results obtained by Yannis and Selcuk have been consistent with this analysis. Furthermore, very long spin coherence times have been demonstrated for deuterons in the COSY storage ring in Juelich, Germany, though only after quite delicate adjustment of nonlinear elements in the ring. Nevertheless COSY is a strong focusing ring for which spin decoherence can be expected to be far greater than in our weak focusing WW-AG-CF lattice.

3 Spin evolution in idealized lattice

Except for idealized specializations, this section reproduces Sections II, III, and IV of Chapter'2 of S.Y. Lee's book "Spin Dynamics and Snakes in Synchrotrons", almost line by line. My purpose is to demonstrate the spectacular simplification that results when the design orbit can be assumed to remain in a single plane. A tiny, but confusing, further alteration is to use y (rather than Lee's z) as vertical coordinate. The coordinates (x, s, y), in (horizontal, longitudinal, vertical) order, (which for Lee is (x, s, z)) will be retained, in spite of the fact that more conventional in the storage ring world would be (horizontal, vertical, longitudinal). This may seem very confusing (partly because the longitudinal Frenet coordinate is to be s) but avoids mis-interpreting z as longitudinal, and it means that, to convert any Lee formula to a formula in this appendix, one only needs to make the replacement $z \to y$ (plus simplifying assumptions). What motivates this coordinate order for spin evolution is that it is useful for the first two coordinates (x, s) as 2D coordinates in the (horizontal) ring design plane, with y being vertical.

3.1 Spin tune

Considering a purely magnetic storage ring, the fundamental BMT spin evolution formula is (SYL-2.40)

$$\frac{d\mathbf{S}}{d\theta} = \mathbf{S} \times \mathbf{F}, \tag{33}$$

where θ is bend angle with $d\theta = ds/\rho$ in a dipole, ρ is radius of curvature, and the applied torque (multiplied by the appropriate factor) is (SYL-2.41)

$$\mathbf{F} = F_x\hat{\mathbf{x}} + F_s\hat{\mathbf{s}} + F_y\hat{\mathbf{y}}. \tag{34}$$

In our idealized ring the design orbit lies in the (x, s) plane and $(y = 0, y' = 0, y'' = 0)$, where derivatives with respect to s are indicated by primes. Using these values, and copying

from (SYL-2.42), the components of $\mathbf{F}$ are

$$\mathbf{F} = \begin{pmatrix} F_x \\ F_s \\ F_y \end{pmatrix} = \begin{pmatrix} 0 \\ 0 \\ -(1+G\gamma) + (1+G\gamma)\rho x'' \end{pmatrix}. \tag{35}$$

Dropping the x'' factor from the only non-vanishing torque can be justified by noting that any deviation x from the appropriate off-momentum closed orbit vanishes on the average. (The validity of this assumption made by S.Y. is reconsidered below.)

Expressing $\mathbf{S}$ in terms of its components (SYL-2.43),

$$\mathbf{S} = S_x\hat{\mathbf{x}} + S_s\hat{\mathbf{s}} + S_y\hat{\mathbf{y}}, \tag{36}$$

and using $d\hat{\mathbf{x}}/d\theta = \hat{\mathbf{s}}$ and $d\hat{\mathbf{s}}/d\theta = -\hat{\mathbf{x}}$ we get (SYL-2.44)

$$\frac{d}{d\theta}\begin{pmatrix} S_x \\ S_s \\ S_y \end{pmatrix} = \begin{pmatrix} (1+F_y)S_s \\ -(1+F_y)S_x \\ 0 \end{pmatrix}. \tag{37}$$

This amounts to being the BMT equation, in S.Y. Lee notation, under our 2D assumptions. Continuing to follow Lee, we define (complex) spin components

$$S_\pm = S_x \pm iS_s, \quad \text{with inverses} \quad S_x = \frac{S_+ + S_-}{2}, \quad S_y = \frac{S_+ - S_-}{2i}, \tag{38}$$

as well as field components $F_\pm = F_x \pm iF_s$ (that will not actually be needed under our special assumptions) to obtain (averaged) equations of motion,

$$\frac{d}{d\theta}\begin{pmatrix} S_\pm \\ S_y \end{pmatrix} = \begin{pmatrix} \pm iG\gamma S_\pm \\ 0 \end{pmatrix}. \tag{39}$$

Solving these differential equations, the spin evolution is given by (SYL-2.45);

$$S_\pm = e^{\pm iG\gamma\theta}S_{\pm 0}, \quad S_y = \text{constant}. \tag{40}$$

One sees that $S_\pm$ are eigenfunctions of the propagation, with eigenvalues $e^{\pm iG\gamma\theta}$. Introduction of $S_\pm$ has further decoupled the spin motion. For propagation around the full ring, one sets $\theta = 2\pi$ and obtains $e^{\pm 2\pi iG\gamma}$ as the eigenvalues. It is because the eigenvalues are complex, while the S_i components are real, that the expansions of eigenfunctions as superpositions of S_i components in Eqs. (38) has required a complex coefficient. On the basis of this solution, for magnetic rings, the spin tune of an "ideal" lattice has been shown to be

$$Q_s = G\gamma. \tag{41}$$

A curious feature of this relation is its lack of dependence on radius of curvature ρ. This came about during the averaging of Eq. (35).

Ordinarily all bending elements are more or less identical and, except for becoming infinite in drift sections, the radius of curvature ρ has roughly the same value everywhere. But one could design a ring where ρ had one value in one sector, and completely different values in

other sectors. This would have no effect on Eq. (41). To say, therefore, that $Q_s = G\gamma$ is a property of an "ideal' lattice, expands dramatically the meaning of "ideal".

A (horizontally) misaligned quadrupole steers the central orbit, but leaves the central closed orbit in the same (horizontal) design plane. Why don't we just pretend that the mis-steering is part of the "design", in which case Q_s is still equal to $G\gamma$. It seems to me, therefore, that Eq. (41) is a global invariant, unaffected by lattice errors, to the extent they leave the central closed orbit in a single plane. (Operationally one always achieves this condition to quite high accuracy.)

It seems, therefore, that the virial theorem calculation can be used to justify S.Y. Lee's earlier dropping of the x'' factor.

Small vertical betatron motion would not alter this conclusion to lowest order. Non-commutation of rotations could violate the averaging to zero, but only proportional to the product of already extremely small amplitudes.

All this is consistent with the earlier 2D virial theorem demonstration that spin decoherence can be neglected in our ultraweak focusing WW-AG-CF lattice. Once a beam bunch has been "captured" its total spin precesses almost as if it were a single particle

3.2 Spinor representation of spin evolution

Continuing to specialize formulas from S.Y. Lee, our Eq. (33) has decoupled to two equations (SYL-2.46)

$$\frac{d\mathbf{S}_\parallel}{d\theta} = G\gamma\,\hat{\mathbf{y}} \times \Big(S_x\hat{\mathbf{x}} + S_s\hat{\mathbf{s}} + S_y\hat{\mathbf{y}}\Big) = G\gamma\Big(S_x\hat{\mathbf{s}} - S_s\hat{\mathbf{x}}\Big), \tag{42}$$

$$\frac{dS_y}{d\theta} = 0. \tag{43}$$

Instead of the 3-component real vectors used so far, one can represent the spin by a 2-complex component general spinor (SYL-2.51),

$$\Psi = \begin{pmatrix} u \\ d \end{pmatrix}. \tag{44}$$

Introducing the Pauli matrices, as the three components of a "vector" $\boldsymbol{\sigma}$,

$$\sigma_x = \begin{pmatrix} 0 & 1 \\ 1 & 0 \end{pmatrix}, \quad \sigma_s = \begin{pmatrix} 0 & -i \\ i & 0 \end{pmatrix}, \quad \sigma_y = \begin{pmatrix} 1 & 0 \\ 0 & -1 \end{pmatrix}. \tag{45}$$

The 3D spin components can be expressed in terms of ψ as (SYL-2.47)

$$S_i = \Psi^\dagger \sigma_i \Psi, \quad \text{for} \quad i = x, s, y. \tag{46}$$

This permits the S_1 components to be expressed in terms of u and d, (SYL-2.52);

$$S_1 = u^* d + u d^*, \quad S_2 = -i(u^* d - u d^*), \quad S_3 = |u|^2 - |d|^2. \tag{47}$$

Even though u and v are complex in general, the S_i components are always real. With this notation, Eq. (42) becomes (SYL-2.48)

$$\frac{d\boldsymbol{\Psi}}{d\theta} = -\frac{1}{2}\,(\boldsymbol{\sigma}\cdot\boldsymbol{\Psi}) = -\frac{i}{2}\,\mathbf{H}\boldsymbol{\Psi}, \quad \text{where} \quad \mathbf{H} = \begin{pmatrix} G\gamma & 0 \\ 0 & -G\gamma \end{pmatrix} = G\gamma\sigma_y. \tag{48}$$

Notice that Lee's perturbation function (SYL-2.49), $\xi(\theta) = F_x(\theta) - iF_s(\theta)$, which would have appeared in the off-diagonal elements of $\mathbf{H}$, actually vanishes identically (as a consequence of our pure-planar design orbit assumption). For a lattice with arbitrary errors the STM formalism continues to be valid, in which case, of course, the off-diagonal elements of $\mathbf{H}$ need to be correctly included.

For initial polarization state $\mathbf{\Psi}(\theta_1)$, solving this differential equation produces a later polarization state $\mathbf{\Psi}(\theta_2)$ given by (SYL-2.54)

$$\mathbf{\Psi}(\theta_2) = e^{-\frac{i}{2}\,\mathbf{H}\,(\theta_2-\theta_1)}\,\mathbf{\Psi}(\theta_1) \equiv t(\theta_2,\theta_1)\,\mathbf{\Psi}(\theta_1). \tag{49}$$

which defines $t(\theta_2, \theta_1)$ as a "spin transfer matrix" (STM) in the spinor formalism. With $\mathbf{H}$ given by Eq. (48), the spin transfer matrix (STM) from θ_1 to θ_2 is given by

$$t(\theta_2,\theta_1) = e^{-\frac{i}{2}\,G\gamma(\theta_2-\theta_1)\,\sigma_y}. \tag{50}$$

This evolution formula resembles Eq. (40) closely, but with the important difference that the matrix σ_y appears here in the exponent. This does not seriously complicate the algebraic manipulations for which results in this appendix are to be applied.

All this "looks like" quantum mechanics, but it has just been mathematical manipulation.

Also important is the one turn transfer map (OTM), $t(\theta)$ from arbitrary initial angle θ, once around the ring and back to the same location. It satisfies (SYL-2.58)

$$\mathbf{\Psi}(\theta+2\pi) = \Pi_{j=1}^{N}\, t(\theta_{j+1},\theta_j)\,\mathbf{\Psi}(\theta), = t(\theta)\,\mathbf{\Psi}(\theta), \tag{51}$$

which concatenates the transfer maps over all N ring sectors starting from θ and returning to the same position.

4 Storage ring as "Penning-Like Trap"

4.1 Motivation

The possibility of storing a large number, such as 10^{10}, of identically polarized particles makes a storage ring an attractive charged particle "trap". But, compared to a table top trap, a storage ring is a quite complicated assemblage of many carefully, but imperfectly, aligned components, powered from not quite identical sources.

For detecting and measuring the EDM of fundamental particles, much has been made of the difficulty imposed by the smallness of their EDM values relative to their MDM values. There is one respect, though, in which it is helpful for the MDM to be "large". It has made it possible for the MDM to have been measured to exquisitely high precision. (Here the phrase "exquisitely high" is being commandeered temporarily as a technical term meaning "can be taken to be exact".) For present purposes the MDM is to be treated as exactly known.

High enough beam polarization, and long enough spin coherence time SCT, make it possible to "freeze" the spins for long enough to attempt to measure the EDM. In this frozen state, the importance of some inevitable machine imperfections, that might otherwise be expected to dominate the errors, is greatly reduced. Examples are beam energy spread and

ring element positioning and alignment uncertainties. (With the benefit of RF-imposed synchrotron oscillation stability) the average beam energy is fixed with the same exquisitely high accuracy with which the MDM is known. The polarization vector serves as the needle of a perfect speedometer. With the RF frequency also known to exquisite accuracy, the revolution period is similarly well known. Then, irrespective of element locations and powering errors, the central orbit circumference is, if not perfectly known, at least very well known. (The minor reservation expressed here is associated with the run-to-run variability associated with possible beam emittance shifts.) An abbreviation intended to encompass all of these considerations will be to refer to the storage ring as a "polarized beam trap".

The precise beam energy determination can be checked occasionally to quite good precision using resonant depolarization Run to run consistency with relative accuracy of 10^{-7} can be expected. Depending on BPM precisions the closed orbit beam orbit positions may be fixed to, perhaps, several micron accuracy at each of the beam position monitors.

Irrespective of the ring circumference, with the beam speed fixed, and the RF period fixed, the closed orbit circumference is known to be constant to arbitrarily high precision. Initially f_0 will be dead-reckoned based on the magic velocity and the nominal ring circumference of the design closed orbit, which is assumed to pass through all element design centers. The actual central closed orbit will not, in fact, pass through these design centers. With actual damping, the central closed orbit would automatically settle nearby. But, even for electrons, the relaxation time is likely to be long compared to the run time, with the effect that the beam never settles into exact equilibrium. To the extent ring lattice elements drift, the bend electric field, and all steering elements will be adjusted to hold the orbit as constant as possible at all beam position monitors (BPM). These adjustments have to be sufficiently adiabatic for the polarization feedback circuits to stay locked. As long as this is satisfied the circumference will never vary

This strategem reduces the importance of some sources of error, but without eliminating them altogether. Of course one will build the EDM storage ring as accurately as possible. But being a "trap" relieves the need for obsessively precise storage ring parameter specifications. For example, r.m.s. element position precision may tentatively be taken to be 0.1 mm, and alignment precision 0.1 milliradian. These are just plausible "place holders" in the present chapter. A real storage ring design will require serious analysis and determination of tolerances like these.

The lack of concern about element absolute positioning must not to be confused as lack of concern for BPM, orbit positioning precision, even assuming the ring has been tuned to be a perfect trap. The direct operational EDM measurement will depend on subtracting results from consecutive pairs of resonator measurements, knowing that only a single control current has been reversed. Precision can be obtained by guaranteeing the forward and reversed beam orbits are identical. With the only intentional change having been a single control current, as few as two BPM's can confirm the symmetry. Better, the symmetry can be monitored as averages over *every* BPM. Micron (10^{-6} m) precision has been achieved, for example in light sources. Commercial BPM's report precision of 1 μm with temperature coefficient less than 1 μm/degree-Celsius. Achieving this level of precision expoits ultrastable circulating beams, such as will be available in EDM rings. Ten or a hundred times better beam positioning accuracy has been claimed for the International Linear Collider collision point optics, even without the benefit of a stable circulating beam.

4.2 Small deviations from magic condition

This section assumes the polarization phase locking described previously has been successful. With the beam polarization locked one can take advantage of the precisely-known electron magnetic moment μ_e and anomalous moment G_e. The spin tune Q_s^E relates to precession around the vertical axis. In an all-electric ring Q_s^E is given by

$$Q_s^E = G_e\gamma - \frac{G_e+1}{\gamma}, \tag{52}$$

For frozen spin electrons at the "magic" value, $Q_s^E = 0$, $\gamma = \gamma_m$, where

$$\gamma_m = \sqrt{\frac{G_e+1}{G_e}} = 29.38243573. \tag{53}$$

Solving Eq. (52) for γ, (and requiring $\gamma > 0$),

$$\gamma = \frac{Q_s^E + \sqrt{Q_s^{E2} + 4G_e(G_e+1)}}{2G_e}, \tag{54}$$

we then obtain

$$\Delta\gamma = \gamma - \gamma_m = \frac{Q_s^E + \sqrt{Q_s^{E2} + 4G_e(G_e+1)}}{2G_e} - \sqrt{\frac{G_e+1}{G_e}}. \tag{55}$$

Though this formula is exact, and quite simple, it can usefully be expanded to

$$\gamma = 29.38243573 + 431.16379, \frac{\Delta f_y}{f_0} + 3163.5\left(\frac{\Delta f_y}{f_0}\right)^2 + \cdots . \tag{56}$$

Here Q_s^E has been re-expressed in terms of the frequency deviation from magic, $\Delta f_y = f_y - f_m$, of the polarization around a vertical axis. This formula is intended for use only near γ_m, with the ratio $\Delta f_y/f_0$ being a tiny number, less than 10^{-5} for example. Further terms are easily obtained, but for values of $\Delta\gamma$ large enough to require them one can simply use Eq. (55). With the RF frequency known to arbitrarily high accuracy and the beam polarization locked to the revolution frequency, measuring the polarimeter response frequency establishes γ to correspondingly high accuracy.

One is accustomed to expecting a spread of spin tunes due to finite betatron and synchrotron amplitudes and energy deviation of each individual particle from the central beam γ value. In a certain sense the beam conditions are better defined than this. As long as decoherence can be neglected (i.e. for times short compared to SCT) the net angular precession of each spin vector cannot exceed $\pi/2$. During this time $\gamma = \gamma_m$ for every particle on the average. One sees that phase locking of the polarization establishes the mean beam parameters to exquisitely high accuracy. Of course this remarkable behavior begins to break down for times approaching SCT. In effect, loss of phase lock and decoherence of the beam polarization are two manifestations of the same spin evolution. Achieving large SCT and maintaining the possibility of phase locking the polarization are equivalent tasks.

This analysis has assumed a purely electric lattice. In practice there will be some average vertical magnetic field component $\langle B_y \rangle$ that will cause the γ value determined by Eq. (56) to be not quite correct. But it has also been anticipated that keeping the polarimeter loop locked will require a Wien filter which compensates for the (unknown) total angular deflection $\Delta\theta_{\rm error}$ by magnetic fields. The spin tune ascribable to this lattice modification is

$$Q_s^{W(\Delta\theta)} = \frac{\Delta\theta_{\rm error}}{2\pi}\left(G_e\gamma - G_e\gamma + \frac{G_e+1}{\gamma}\right) \approx \frac{\Delta\theta}{2\pi}\frac{G_e+1}{\gamma_m} = \frac{\Delta\theta_{\rm error}}{2\pi}\frac{1.00116}{29.38243}. \qquad (57)$$

which compensates for fraction $\Delta\theta_{\rm error}/(2\pi)$ of each turn being caused by magnetic rather than electric field. The (well, but not perfectly, known) strength I_x^W of the Wien filter excitation can be interpreted as a measurement of the angular bend caused by unknown magnetic field component $\langle B_y \rangle$ averaged over the ring. The ultimate claimed γ precision depends on this correction. In the actual experiment, since the roll is around the radial axis, the spin tune will necessarily be exactly zero, meaning the phase locking requires the Wien filter to exactly cancel $\langle B_y \rangle$.

One problematical phase-locked loop detail concerns the "polarity reversal" performed to isolate the EDM contribution. It would be splendid if the roll reversal could be completed without losing phase lock. But reversing the roll introduces a discontinuous phase shift in the polarization signal inputs to the resonant polarimeters which will force the circuits to ring down and then ring up again, unlocking the closed loop synchronization.

Perhaps the roll drive phase could be judiciously reversed at just the right time to avoid this effect and preserve all phase locking? If this could be done then the roll orientation could be reversed at a quite high rate within each fill cycle, greatly reducing systematic frequency shift errors. If not, then roll reversal may have to be limited to once per fill. However there is an excellent reason for *not* attempting to synchronize any control function with the roll frequency—it would contradict the claim made earlier in the paper that no control sources are synchronous with the roll frequency. Violating this seems sure to cause trouble. This seems to guarantee loss of phase-lock during roll reversal.

5 Pseudo-frozen spin magnetic lattice possibilities, for e, p, d and He^3 particles

Because the EDM effect is so small, one seeks a configuration in which the EDM torque is being applied almost all the time, and its effect is monotonic—constructively building up the EDM-induced precession. Ideally the EDM torque present in each of the bending elements in the ring would have this property. (Othherwise any EDM accumulation would be limited to a small sector of the ring, and would be proportionally weaker.) Fully constructive accumulation would requires the spin tune to vanish. This is a necessary, but not necessarily sufficient, condition for fully constructive EDM accumulation.

Figure 2 provides plots of magnetic lattice tunes for protons, deuterons, helions, and electrons, with integer and half integer crossings emphasized. There is no case for which the spin tune vanishes. This prevents any EDM-induced precession occurring in the bending magnets from accumulating constructively to give an EDM signal proportional to the run

duration. Table 1 contrains some of the pseudo-frozen spin possibilities for the four particle types.

Table 1: Candidate magic energies for magnetic ring pseudo-frozen spin operation. Particles considered are protons, deuterons, helium-3, and electrons. OTM is "one-turn-map" and STM is "spin transfer matrix". Q_{s0} is the uncorrected spin tune (read from Figure 2). N_S is a canditate number of equal-strength solenoidal snakes (of arbitrary sign) capable of adjusting the spin tune to zero. (Just for this table) R represents the STM for spin precession through π/N_S around the vertical ($\hat{\mathbf{y}}$) axis, and S represents the STM for a single solenoid (of either sign) snake, that rotates each spin vector through angle $\pm\pi$ around the local longitudinal ($\hat{\mathbf{s}}$) axis. Useful abbreviation: $(RSR)^2 \equiv RSR \cdot RSR$, etc. The deuteron case is, because of its high energy requirement, is, by far, the least promising case. For the electron there are higher pseudo-frozen energies, needing only achievably strong solenoid snakes. Entries in the OTM column indicate there is a figure in the next section showing spin evolution around such a ring.

	pc or E		unit	Q_{s0}	OTM	solenoid π-snake strength, [T-m]
p	465	pc	MeV	2.0		4.88
	907			2.5		9.52
	1251			3.0		13.12
d	6.43	pc	GeV	-0.5		57.7
He3	1118	pc	MeV	-4.5		18.6
	1825			-5.0		30.4
e	220	E	MeV	0.5	RSR,$(RSR)^2$	2.31
	440			1.0	RSR,$(RSR)^2$	4.62
	661			1.5		6.93
	881			2.0		9.24

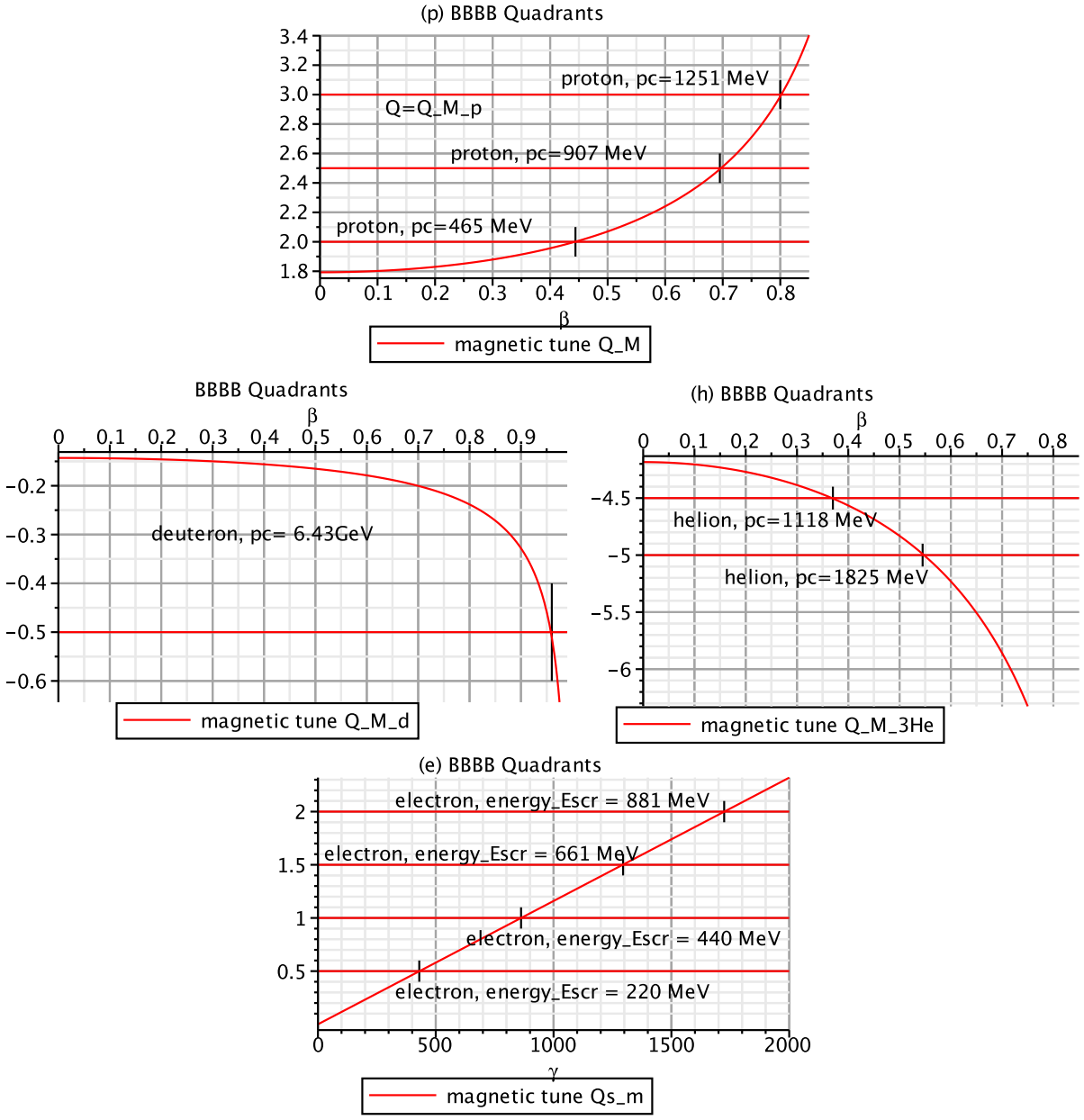

Figure 2: Magnetic lattice spin tunes for protons, deuterons, helions, and electrons.

A natural question, then, is whether Siberian snakes included in the ring can have the property of shifting the spin tune to zero. The following figures show that this can, in fact, be accomplished. So $Q_s = 0$ can be achieved in a magnetic lattice with Siberian snakes.

Unfortunately, subsequent figures will show, that monotonic EDM-induced precession still does not occur. Since each snake reverses the accumulated EDM precession, it is clear that an even number of snakes is required. When the snakes are uniformly distributed the spins can be frozen, but there is no net EDM effect per turn. And with the snakes non-uniformly distributed the spins cannot be frozen.

6 Spin tune alteration using Siberian snakes

6.1 Can pseudo-frozen spin be made global? Yes.

From the previous figures it can be seen that there are no examples for which the spin tune vanishes in a magnetic ring. One can investigate whether Siberian snakes can be used to produce truly global frozen spin operation in a magnetic ring such as COSY, in spite of the fact that there are no examples for which the spin tune vanishes.

Can one design a magnetic ring that includes (longitudinal) solenoidal Siberian snakes and has the property that a particle starting with spin pointed in the forward hemisphere, remains for ever with spin pointed into the forward hemisphere. In other words, can the spin tune be arranged to vanishe?. The effect of any non-zero EDM would tend then, always, to tip the spin out of the plane, say up, as it passes through each bending magnet.

Figures below show that the $Q_s = 0$ can, in fact, be achieved using Siberian snakes.

6.2 Can snakes enable EDM measurement in magnetic ring? No.

Regrettably, Figures 3, 4, and 5 with, respectively, one, two, or four snakes, show that the Siberian snakes invariably have the effect of flipping any pre-existing EDM-induced spin precession. This prevents any systematic accumulation of EDM signal over multiple turns around any purely magnetic storage ring.

By superimposing electric and magnetic it is theoretically easy to produce a frozen spin lattice for any charged fundamental particle without using Siberian snakes. As a practical matter though, it is extremely difficult, experimentally, to superimpose the required extremely strong electric field on even a weak magnetic field.

To avoid this impediment one can contemplate a ring in which some sectors are magnetic, and others electric. Regrettably, this option is probably not satisfactory. Inevitably, element placement and powering errors introduce spin precession errors. To the extent all precessions leave the spins in the same horizontal plane separating electric and magnetic bending would probably be satisfactory. because rotations about the same axis commute, and these spurious rotations would tend to cancel.

But precessions around different axes. When passing through, say, an electric bend sector, three significant precessions will have accumulated, a large spin tune precession, a small element error precession, and a small EDM-induced precession. Failure of commutation

of successive rotations will tangle these precessions enough to make it impossible to isolate the desired EDM contribution.

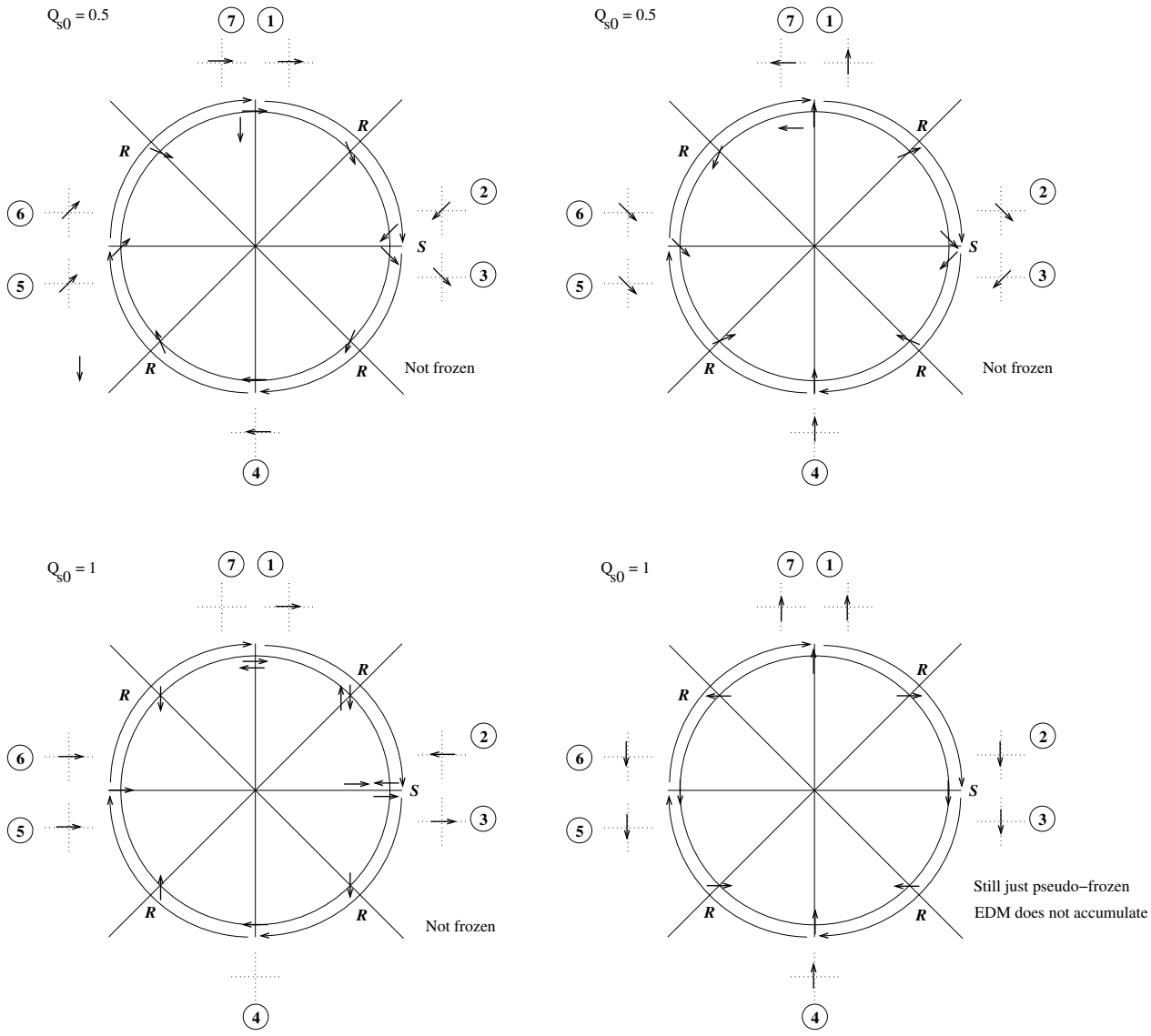

Figure 3: Some single snake possibilities for frozen spin modification of a magnetic ring using helical snakes. Snake locations are indicated by "S", natural spin tune precession by "R". Even in cases with the spins (essentially) frozen, $Q_s = 0$, the snake toogles any EDM precession, which prevents the build-up of any EDM signal.

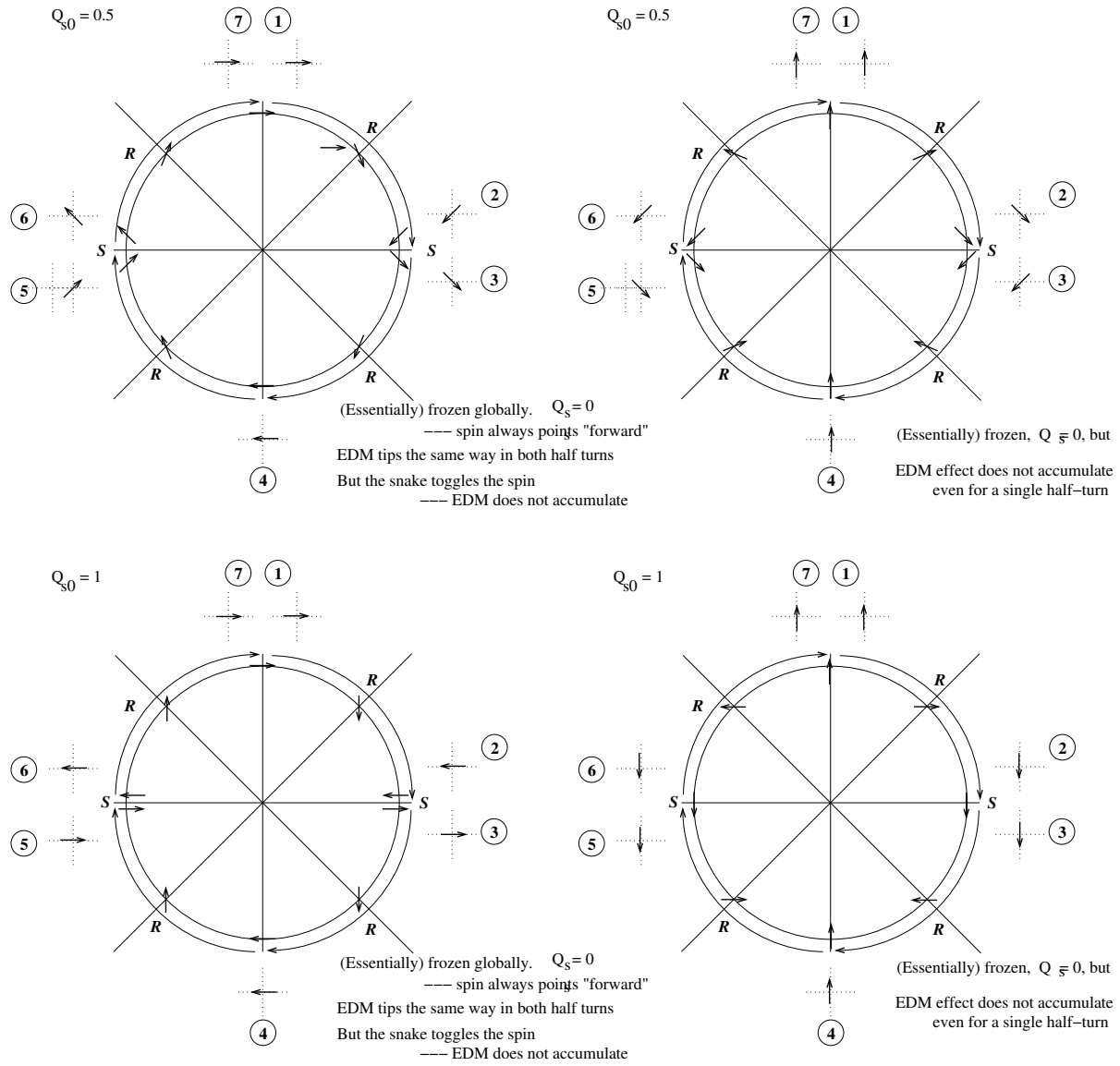

Figure 4: Some two snake possibilities for frozen spin modification of a magnetic ring using helical snakes. Snake locations are indicated by "S", natural spin tune precession by "R". For $Q_s = 1$, with no snakes, an initially forward-pointed spin would only be "pseudo-frozen", pointing forward again at the origin, but also half way aroung the ring. $Q_s = 0.5$, with no snakes, a initially forward-pointed spin, precesses through π after one turn, and is forward-pointed again after two turns. Even in cases with snakes (essentially) freezing the spins to $Q_s = 0$, the snakes toogle any EDM precession, which prevents the build-up of any EDM signal.

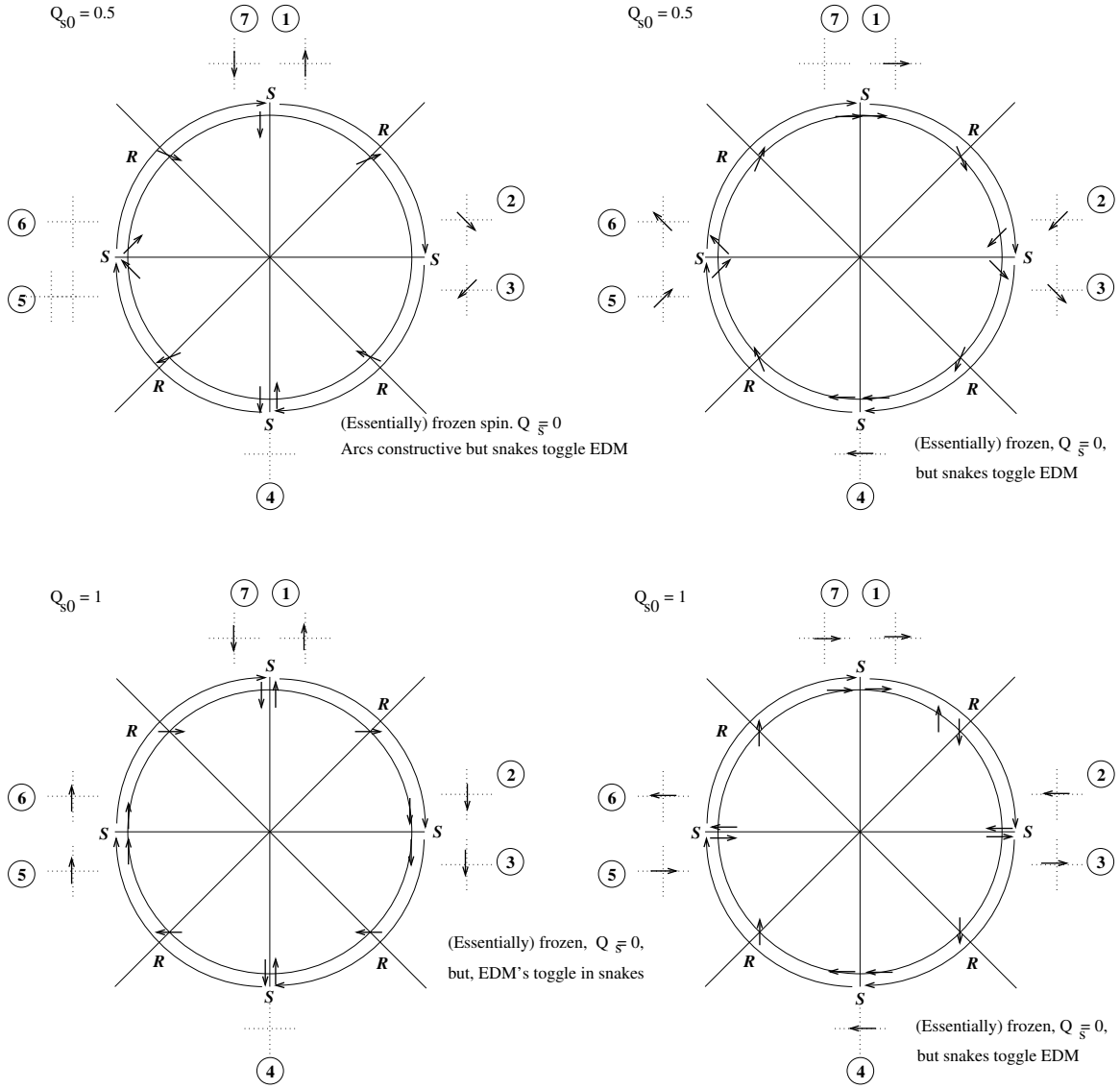

Figure 5: Some four snake possibilities for frozen spin modification of a magnetic ring using helical snakes. Snake locations are indicated by "S", natural spin tune precession by "R". Even in cases with the spins (essentially) frozen, $Q_s = 0$, the snakes toogle any EDM precession, which prevents the build-up of any EDM signal.

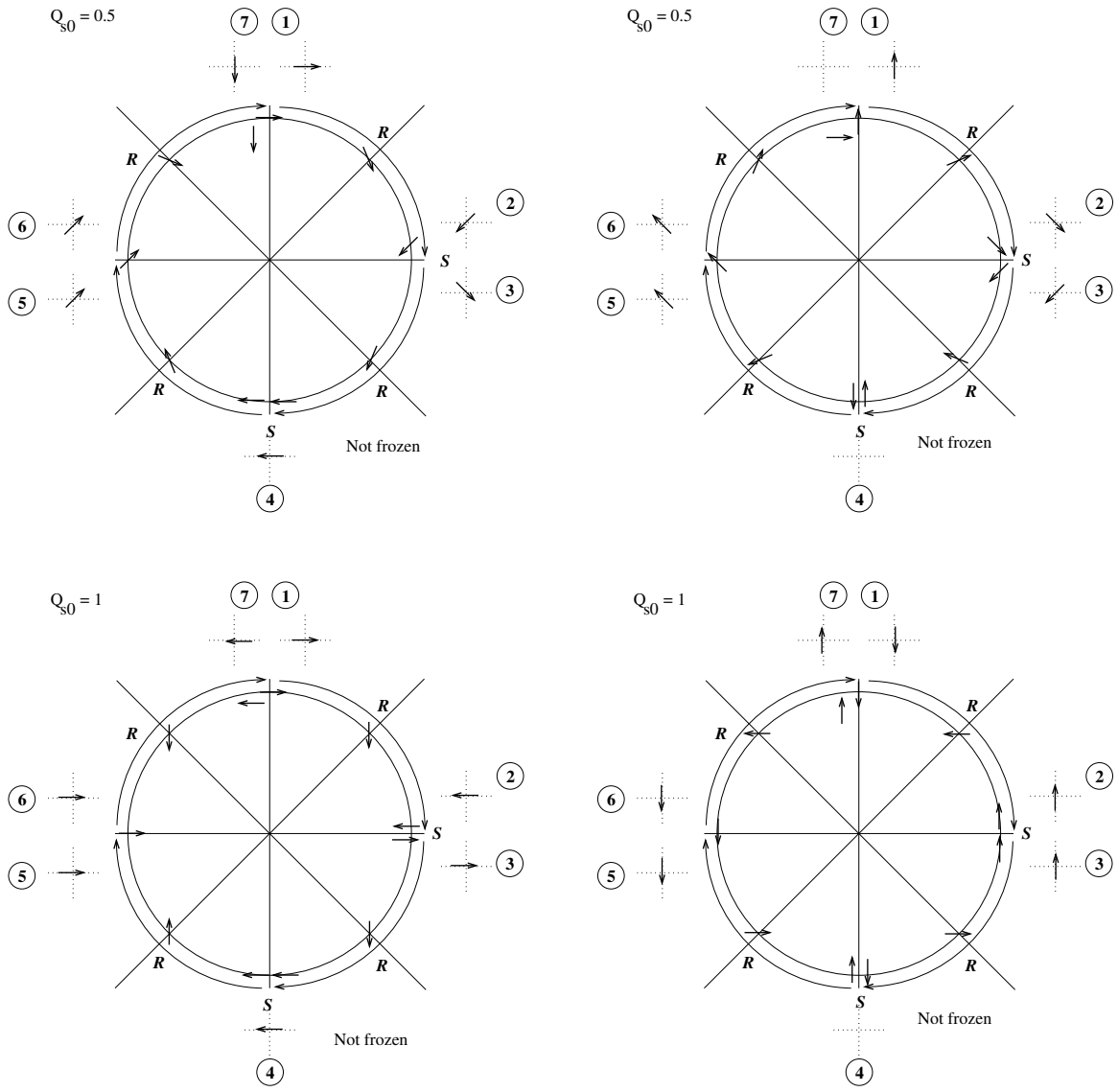

Figure 6: To prevent toggling of the EDM signal there must be an even number of snakes. Furthermore they must be "unbalanced" as in this figure. However, since there is no frozen spin case, there is no EDM candidate.

APPENDICES

A Spin evolution through non-bend elements

A.1 Spin evolution through fringe fields

To account for the effect of bending element end fields, incremental precessions have to be included at entrance and exit. Certainly, averaged over time, the sum of all design field bend angles, including bending in fringe fields, has to be 2π. In a "hard edge" the sum of the design bend angles has, presumably, been adjusted to 2π. Furthermore, the fringe field precession on the design orbit is assumed to vanish. The residual fringe electric field is bipolar. For the ultraweak focusing WW-AG-CF ring we know that all inside velocities can be taken to be magic. It is shown later that, even including betatron oscillations, no net decoherence occurs in the bend regions. There is, howeveer, a tendency for over-momentum particles (the ones that tend to be closer to the outer electrode) under-precess because they are more over-momentum in the outer-region part of the fringe field, where the electric field has sign opposite to the main bend field. Nevertheless, averaged over a single synchrotron oscillation cycle, there is a strong tendency for this source of decoherence to cancel. One can, however, estimate the accuracy with which this averaging has to be tailored.

As a particle enters or exits a bend element, its potential energy can be approximated as changing discontinuously with its kinetic energy changing correspondingly. Especially with decoherence being so nearly negligible in bend fields for which the field index m is so close to 1, we have to treat fringe field regions very carefully. Instead of treating the potential as discontinuous, we now assume the change occurs over a longitudinal distance $\Delta z^{\rm FF}$ which, for estimation purposes, we take equal to the separation distance between the electrodes; $\Delta z = g_{\rm gap}$. (For an idealized "toy" model introduced later, with the drift lengths taken to be zero, fringe field spin precession can be neglected.) The fringe field region is assumed to be short enough to be treated as "thin". That is, any change in the particle's radial offset occuring in range Δz is to be neglected and the integrated deflection applied at the center (i.e. at the bend edge). As a result the curve $x(z)$ is continuous, but its slope dx/dz is discontinuous. Entrance transitions from outside a bend to inside are described first.

Inside the bending element the increase in potential energy from orbit centerline to radial position x is $e\Delta V(x)$. As synchroton oscillations move the particle radially in and out, the sign of $\Delta V(x)$, just inside the bend edge oscillates between negative and positive values, and the sign of the deviation from the magic velocity oscillates correspondingly. This will tend to average away the spin run-out occurring in the fringe field region over times long compared to the synchrotron period. In the long run it is the deviation from zero of this average that has to be determined.

Supposing there are 20 bend elements, and the length of the fringe field region is equal to the gap thickness $g_{\rm gap} = 0.03\,{\rm m}$, the deflection angle $\theta^{(FF)}$ of the design orbit in the fringe field at one such edge is approximately

$$\theta^{(FF)} \approx \frac{1}{2}\,\frac{\Delta z^{\rm FF}}{r_0} \quad \Big(\stackrel{\rm e.g.}{=} 0.5 \times 0.03/40 = 0.375 \times 10^{-3} \Big). \tag{58}$$

This is half of the deflection occurring in advancing a distance $g_{\rm gap}$ in the interior of the bend. (The angle $\theta^{(FF)}$ is implicitly assumed to be positive, irrespective of whether the orbit is clockwise or counter-clockwise.) Consider a particle approaching the fringe field region at radial displacement x. At the longitudinal center of the fringe field region the kinetic energy of this particle deviates from its "proper" (i.e. fully-inside value at radial displacement x) by the amount

$$\Delta\gamma^{(FF)}(x) \approx \frac{1}{2}\,\frac{\Delta V(x)}{m_p c^2/e} \approx \frac{1}{2}\,\frac{E\,x}{m_p c^2/e}, \tag{59}$$

where $\Delta V_{\rm tot}$ is the total voltage increase from inner electrode to outer electrode. (The electric field points radially inward in order for positive particles to bend toward negative x but, by convention, E is positive.) Here, for simplicity, we are neglecting the fact that the actual electric field will have more complicated x-dependence depending, for example, on the value of the field index m. Our assumed fringe field spatial dependence is also simplistic.

According to Eq. (16) the leading effect of passage through a bend region with γ deviation from magic $\Delta\gamma$, is a rate of change of spin angle α per unit deflection angle θ given by

$$\frac{d\alpha}{d\theta} \approx \left(\frac{g}{2} - 1 + \frac{g/2}{\gamma_0^2}\right)\Delta\gamma \quad \left(\stackrel{\text{for proton}}{=} 3.586\,\Delta\gamma.\right) \tag{60}$$

Combining equations, the excess angular advance occurring while entering the bend at displacement x is

$$\boxed{\widetilde{\Delta\alpha}^{\rm FF} = +\left(\frac{g}{2} - 1 + \frac{g/2}{\gamma_0^2}\right)\frac{1}{2}\,\frac{E\,x}{m_p c^2/e}\,\theta^{FF}.} \tag{61}$$

It is worth noting that, unlike the similar looking (but nearly vanishing) factor in Eq. (16), the second sign in factor $(g/2-1+g/(2\gamma_0^2))$ is positive, rather than negative. Instead of vanishing, the terms in this factor therefore sum constructively. (**Aside:** it may be appropriate to keep another term in expansion (60) in order to include the effect that dispersion introduces a correlation between γ and x which, after averaging, leaves a finite precession, even if $< x >$ vanishes in Eq. (61) .)

In our treatment of this edge effect we are assuming this precession lies in exactly the same plane as the orbit plane of the particle in the bend element, justifying the notation $\widetilde{\Delta\alpha}^{\rm FF}$ Entrance (and, later, exit) values can simply be added to the main precession through the bend element. Meanwhile, in the fringe field region the advance of the tangent to the orbit is $\theta^{(FF)}$ as given by Eq. (58). The + sign on the rhs of Eq. (61) reflects the fact that, for a particle displaced radially outward, the particle momentum is completing some of its rotation in the fringe field where its magnitude is more positive than in the bend interior.

Though the fringe field precession occurs continuously over the range $g_{\rm gap}$ it is applied discontinuously at the bend edge. This is consistent with our hard edge treatment of the particle's momentum evolution. Because $\widetilde{\alpha}$ is measured relative to the orbit direction, Eq. (61) gives the spin angle precession over and above the advance of the tangent to the orbit.

The fact that spin and momentum angular advances do not match has come about because the particle has bent appreciably while its speed deviates from the magic value. On exiting the bend element the particle also bends appreciably while its γ deviation is given by the same formula (59). Eq. (61) therefore applies to both entrance and exit. Unfortunately

this means that excess input precession and excess output precession combine constructively rather than tending to cancel (as edge field orbit focusing typically does.)

The largest magnitude $\Delta\gamma^{(FF)}$ can have is

$$|\Delta\gamma^{(FF)}_{\max}| = \frac{1}{4}\,\frac{E\,g_{\rm gap}}{m_p c^2/e} \quad \left(\stackrel{\text{e.g.}}{=} \frac{1}{4}\,\frac{(10.5\times10^6)\times 0.03}{0.938\times10^9} = 0.84\times10^{-4}.\right) \tag{62}$$

For a particle with magic velocity skimming the outer electrode, where the effect is maximum, the angular runout is given by

$$\begin{aligned} |\Delta\alpha^{(FF)}_{\max}| &\approx \left(\frac{g}{2} - 1 + \frac{g/2}{\gamma_0^2}\right)\Delta\gamma_{\max}\,\Delta\theta^{(FF)} \\ &= 3.586\times(0.84\times10^{-4})\times(0.375\times10^{-3}) \\ &= 1.13\times10^{-7}\,\text{radians/edge}. \end{aligned} \tag{63}$$

With perhaps 50 edges in the lattice, and revolution frequency of about 1 MHz, the maximum spin runout could be as much as one revolution per second. This vastly exaggerates the spin decoherence, of course, because it does not account for the averaging effect of synchrotron oscillations. A challenge for lattice design is to perfect the synchrotron oscillation averaging to cancel this source of spin decoherence. Since synchrotron oscillations are usually at least somewhat nonlinear this averaging is not automatic. This source of decoherence can, however, be tuned away operationally by tailoring the synchrotron oscillations. So I neglect this source of decoherence.

A.2 Non-bend elements

Some elements (especially quadrupoles) can cause vertical deflections which alter s_y. Being proportional to transverse displacements these deflections are very small and tending to cancel because of their alternating polarity. Nevertheless it is necessary to keep track of their effects.

On an element-by-element basis, when a particle has just entered an element that bends (for example) in a plane rolled counter-clockwise by angle ϕ about the z-axis, it is first necessary to transform its laboratory frame coordinates (s_x, s_y, s_z) into bend frame coordinates $(\tilde{s}_x, \tilde{s}_y, \tilde{s}_z)$ using

$$\begin{pmatrix}\tilde{s}_x\\ \tilde{s}_y\\ \tilde{s}_z\end{pmatrix} = \begin{pmatrix}\cos\phi & -\sin\phi & 0\\ \sin\phi & \cos\phi & 0\\ 0 & 0 & 1\end{pmatrix}\begin{pmatrix}s_x\\ s_y\\ s_z\end{pmatrix} \tag{64}$$

(As it stands, this equation is over-simplified since (in the presence of vertical betatron oscillation) the normal to the bend plane can have a (tiny) component along the longitudinal axis. This complication is being ignored in the present discussion.) The roll angle ϕ has been chosen so that the element causes pure precession through some calculable angle $\widetilde{\Delta\alpha}$ about some known axis. With the particle speed known, $\widetilde{\Delta\alpha}$ is determined unambiguously by the (known) magnitude of the angular deflection in the multipole element. The plane of deflection is also available from the particle tracking through the element. Expressing the

spin precession also by a 3×3 matrix, and transforming back to the erect laboratory frame, one obtains the new cartesian components,

$$\begin{pmatrix} s_x \\ s_y \\ s_z \end{pmatrix}_{\text{after}} = \begin{pmatrix} \cos\phi & \sin\phi & 0 \\ -\sin\phi & \cos\phi & 0 \\ 0 & 0 & 1 \end{pmatrix} \begin{pmatrix} \cos\widetilde{\Delta\alpha} & 0 & -\sin\widetilde{\Delta\alpha} \\ 0 & 1 & 0 \\ \sin\widetilde{\Delta\alpha} & 0 & \cos\widetilde{\Delta\alpha} \end{pmatrix} \begin{pmatrix} \cos\phi & -\sin\phi & 0 \\ \sin\phi & \cos\phi & 0 \\ 0 & 0 & 1 \end{pmatrix} \begin{pmatrix} s_x \\ s_y \\ s_z \end{pmatrix}_{\text{before}} \tag{65}$$

In an actual tracking program, for improved numerical presision, matrix products like these should be explicitly concatenated in closed form, with all elements expressed as (rapidly convergent) truncated expansions in products of (small) angles and (small) precession angle $\widetilde{\Delta\alpha}$. The resultant matrix differs from the identity matrix only by differentially-small, rapidly-convergent elements. The purpose for this maneuver is to avoid loss of accuracy in relying on numerically evaluated differences of almost equal quantities. This step is important in preventing the tracking precision from being limited by computer machine precision. This suppresses one possible source of spurious damping or anti-damping.

A.3 Spin evolution through miscellaneous thin elements

In principle the only lattice elements in the proposed proton EDM lattice design are bends and drifts. Spin evolution through these elements has already been discussed. All other elements are to be treated as thin element kicks. Rearranging Eq. (60) produces, for spin evolution through a thin element,

$$\boxed{|\widetilde{\Delta\alpha}| \approx \left(\frac{g}{2} - 1 + \frac{g/2}{\gamma_0^2}\right) \Delta\gamma\, \widetilde{\Delta\theta}} \tag{66}$$

where $\widetilde{\Delta\theta}$ is positive by definition and $\widetilde{\Delta\alpha}$ is the angular deviation of the bend plane spin coordinate relative to the orbit. The absolute value sign in this equation eventually has to be removed; it is included here so that the discussion of signs can be deferred. In paraxial approximation, for a particle with transverse position (x, y), the magnitude of the (not necessarily horizontal) angular deviation $\widetilde{\Delta\theta}$ in a quadrupole of strength q is given by

$$\widetilde{\Delta\theta} = |q|\sqrt{x^2 + y^2}, \tag{67}$$

where q is the inverse focal length of the quadrupole.

The magnitude of the angular deflections in sextupoles and higher order multipoles are also functions only of the combination $r = \sqrt{x^2 + y^2}$. Eq. (67) generalizes to

$$\begin{aligned} \widetilde{\Delta\theta}_{\text{quad}} &= |q| r, \\ \widetilde{\Delta\theta}_{\text{sext}} &= \frac{|S|}{2}\, r, \\ \widetilde{\Delta\theta}_{\text{oct}} &= \frac{|O|}{6}\, r, \end{aligned} \tag{68}$$

where S is the conventionally defined sextupole strength and O is the conventionally defined octupole strength. The element strengths appearing in an SXF lattice description file include

the numerical factors. That is, the quad parameter is $b_1 = q$, the sextupole parameter is $b_2 = S/2$, the octupole parameter is $b_3 = S/6$, and so on.

A significant complication concerns the sign of the $\widetilde{\Delta\alpha}$. For a particle with no vertical displacement there is no ambiguity, since the bend plane in the quadrupole is the same as the overall (horizontal) lattice design plane. In this case, with $y = 0$, Eq. (66) can be made more explicit;

$$\widetilde{\Delta\alpha_h} \approx \left(\frac{g}{2} - 1 + \frac{g/2}{\gamma_0^2}\right) \Delta\gamma \, q \, x. \tag{69}$$

where, by convention, a horizontal *focusing* quad has $q > 0$. The sign in Eq. (69) reflects the fact that, for $x > 0$ and $q > 0$, the quadrupole "helps" by bending the momentum in the same sense as the bending elements. This formula makes it clear that reversing the sign of q reverses the sign of $\widetilde{\Delta\alpha}$.

For obtaining the proper sign for vertically focusing quadrupoles it is necessary to handle consistently the transformation from laboratory to bend frame spin coordinates, which is why the sign issue has been deferred until after discussing this transformation.

Most of the elements in a storage ring cause spin precession which approximately conserves the vertical component of spin $s_y\hat{\mathbf{y}}$. The leading exceptions to this in a proton EDM storage rings are the vertically focusing or defocusing quadrupoles present in the lattice to keep β_x magnageably small. Particles having non-vanishing vertical betatron amplitude are deflected vertically which causes $s_y\hat{\mathbf{y}}$ to precess. (As an aside it can be mentioned that there is a very strong tendency for this precession to cancel in subsequent quadrupoles and, therefore, probably not contribute significantly to spin decoherence. Nevertheless it is important for the precession to be modeled correctly.) All quadrupoles and sextupoles in the lattice cause similar precession to at least some degree.

The planes of deflection for particles incident on a quadrupole are shown in Figure 7. In a perfect multipole field the magnitude of the total deflection angle is constant on a contour of fixed radius (i.e. a circle centered on the origin.) For a particle incident at (x_0, y_0) the equation of the line of intersection of the deflection plane with the transverse plane is

$$y = y_0 - \frac{y_0}{x_0}\,(y - y_0), \tag{70}$$

As shown if the figure, the roll-angle of the deflection plane (with counter-clockwise roll taken as positive) is $\phi_0 = \tan^{-1}(y_0/x_0)$, irrespective of quadrant and whether the quadrupole is focusing or defocusing. However the inverse tangent function is, itself, multiple valued. To make it single valued one can determine ϕ_0 using

$$\phi_0 = \arctan2(qy_0, qx_0). \tag{71}$$

Along with Eq. (66), this establishes both the sign and magnitude of $\widetilde{\Delta\alpha}$, while preserving the sign reversal when the sign of q reverses. This should be checked numerically in all quadrants. For sextupoles, octupoles and other multipoles it is also necessary to generalize Eq. (71). Figure 8 is intended to be helpful. The results are

$$\begin{aligned} \phi_{0,\mathrm{quad}} &= 1\arctan2(qy_0, qx_0), \\ \phi_{0,\mathrm{sext}} &= 2\arctan2(Sy_0, Sx_0), \\ \phi_{0,\mathrm{oct}} &= 3\arctan2(Oy_0, Ox_0). \end{aligned} \tag{72}$$

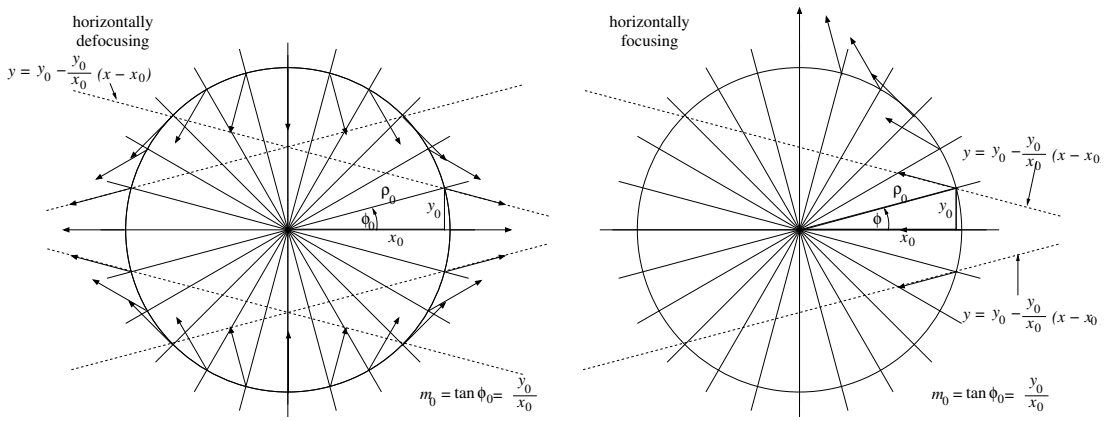

Figure 7: The broken lines shows the deflection planes for particle with dispacements x_0, y_0 in various quadrants, incident on an erect quadrupole. The roll-angle of the deflection plane (with counter-clockwise roll taken as positive) is $\phi_0 = \tan^{-1}(y_0/x_0)$ irrespective of quadrant, and irrespective of whether the quadrupole is focusing or defocusing.

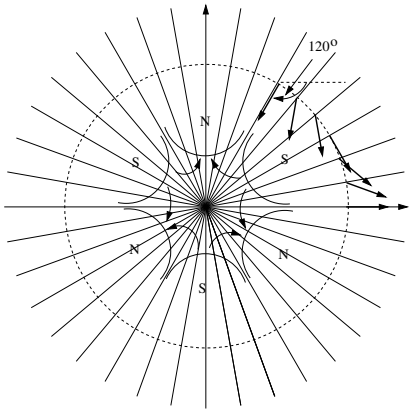

Figure 8: Pole profiles for a sextupole element are shown. By comparison with Figure 7, this figure is intended to help in generalizing Eq. (71) to sextupoles, octupoles, and other multipoles.

With roll angles of the bend plane determined this way, the following formulas apply to all multipoles.

Substitution into Eq. (65) and setting $\phi_0 = \phi$ produces

$$\begin{pmatrix} s''_x \\ s''_y \\ s''_z \end{pmatrix} = \begin{pmatrix} \cos\phi & \sin\phi & 0 \\ -\sin\phi & \cos\phi & 0 \\ 0 & 0 & 1 \end{pmatrix} \begin{pmatrix} \cos\widetilde{\Delta\alpha} & 0 & -\sin\widetilde{\Delta\alpha} \\ 0 & 1 & 0 \\ \sin\widetilde{\Delta\alpha} & 0 & \cos\widetilde{\Delta\alpha} \end{pmatrix} \begin{pmatrix} \cos\phi & -\sin\phi & 0 \\ \sin\phi & \cos\phi & 0 \\ 0 & 0 & 1 \end{pmatrix} \begin{pmatrix} s_x \\ s_y \\ s_z \end{pmatrix} \quad (73)$$

It is appropriate, to improve numerical precision, to break the central matrix into two terms, $\mathbf{I} + \mathbf{\Delta}$ where $\mathbf{I}$ is the identity matrix and $\mathbf{\Delta}$ is a small deviation. Then, since $\mathbf{I}$ commutes with the outer matrices, and their product is $\mathbf{I}$, the final result is equal to $\mathbf{I}$ plus a small deviation. Calculation of the *changes* in spin coordinates requires only the term proportional

to $\sin(\widetilde{\Delta\alpha}$, which is

$$2\sin(\widetilde{\Delta\alpha}/2)\begin{pmatrix} -\cos(\phi)^2\sin(\widetilde{\Delta\alpha}/2) & \cos(\phi)\sin(\widetilde{\Delta\alpha}/2)\sin(\phi) & -\cos(\phi)\cos(\widetilde{\Delta\alpha}/2) \\ \cos(\phi)\sin(\widetilde{\Delta\alpha}/2)\sin(\phi) & -\sin(\phi)^2\sin(\widetilde{\Delta\alpha}/2) & \sin(\phi)\cos(\widetilde{\Delta\alpha}/2) \\ \cos(\phi)\cos(\widetilde{\Delta\alpha}/2) & -\sin(\phi)\cos(\widetilde{\Delta\alpha}/2) & -\sin(\widetilde{\Delta\alpha}/2) \end{pmatrix}. \tag{74}$$

As mentioned before, all components in this matrix are small, of order $\widetilde{\Delta\alpha}$ or smaller, even if the angle ϕ is as great as $\pi/2$. Multiplying this matrix on the right by $(s_x, s_y, s_z)^T$ produces deviations $(\Delta s_x, \Delta s_y, \Delta s_z)$ which, added to (s_x, s_y, s_z), give the output spin coordinates.

B Spin tunes

B.1 Field Transformations

The dominant fields in an electric storage ring are radial lab frame electric $-E\hat{\mathbf{x}}$ and/or vertical lab magnetic field $B\hat{\mathbf{y}}$. They give transverse electron rest frame field vectors $\mathbf{E}'$ and $\mathbf{B}'$, and longitudinal electric and magnetic components E'_z and B'_z, all related by

$$\mathbf{E}' = \gamma(\mathbf{E} + \beta \times c\mathbf{B}) = -\gamma(E + \beta cB)\,\hat{\mathbf{x}} \tag{75}$$

$$\mathbf{B}' = \gamma(\mathbf{B} - \beta \times \mathbf{E}/c) = \gamma(B + \beta E/c)\,\hat{\mathbf{y}} \tag{76}$$

$$E'_z = E_z, \tag{77}$$

$$B'_z = B_z. \tag{78}$$

B.2 MDM-Induced Precession in Electric Field

A particle in its rest system, with angular momentum $\mathbf{s}'$ and magnetic dipole moment $g\mu\mathbf{s}'$, in magnetic field $\mathbf{B}'$, is subject to torque $g\mu\mathbf{s}' \times \mathbf{B}'$. Here $\mu = e\hbar/(2m)$ is the "magneton" value for a particle of that particular mass and charge. By Newton's angular equation, substituting from Eq. (76) to express the fields in laboratory coordinates,

$$\frac{d\mathbf{s}'}{dt'} = -g\mu\mathbf{B}' \times \mathbf{s}' = -g\mu\gamma\Big(B + \beta\,\frac{E}{c}\Big)\,\hat{\mathbf{y}} \times \mathbf{s}'. \tag{79}$$

In the customary "mixed-frame" notation, the rest frame angular momentum is represented by $\mathbf{s}$ rather than by $\mathbf{s}'$ (because $\mathbf{s}$ is defined to be a true 3-vector only in that frame) and the laboratory time interval $dt = dt'\gamma$ is used instead of rest frame time interval dt'. Furthermore, the magnitude $|\mathbf{s}|$ is known to be constant. With the laboratory field being purely electric and purely radial, the vertical component of $\mathbf{s}$ is conserved. The normalized horizontal component $\hat{\mathbf{s}}$ satisfies

$$\frac{d\hat{\mathbf{s}}}{dt} = -\frac{g}{2}\,2\mu\beta\,\frac{E}{c}\,\hat{\mathbf{y}} \times \hat{\mathbf{s}}. \tag{80}$$

As Jackson explains, for accelerated motion, for example circular, relativistic effects cause the electron axis to precess in the laboratory, irrespective of any static moments the electron may have. This Thomas precession causes the polarization vector to precess even if there is no torque acting on the magnetic or electric moments. This precession has to be allowed for

when ascribing precession to MDM's or EDM's. In our case, the beam direction advances uniformly, by 2π during one revolution period $T_{\rm lab}$ and the Thomas precession totque term is

$$\frac{\gamma-1}{v^2}\left(\frac{d\mathbf{v}}{dt}\times\mathbf{v}\right)\times\hat{\mathbf{s}}=\frac{\gamma-1}{v^2}\left(\frac{-\hat{\mathbf{x}}v^2}{r_0}\times\mathbf{v}\right)\times\hat{\mathbf{s}}$$
$$=\frac{\gamma-1}{r_0/v}\,\hat{\mathbf{y}}\times\hat{\mathbf{s}}=\left(1-\frac{1}{\gamma}\right)2\mu\,\frac{E/c}{\beta}\,\hat{\mathbf{y}}\times\hat{\mathbf{s}}. \tag{81}$$

Adding this term to the electric part on the rhs of Eq. (79),

$$\frac{d\hat{\mathbf{s}}}{dt}\Big|_{\rm MDM,E}=2\mu\Big(-\frac{g}{2}+\frac{\gamma}{\gamma+1}\Big)\,\beta\frac{E}{c}\,\hat{\mathbf{y}}\times\hat{\mathbf{s}}. \tag{82}$$

This agrees with Jackson's Eq. (11.170). We try a solution of the form

$$\hat{\mathbf{s}}_{\rm MDM,E}=\big(\hat{\mathbf{Z}}\,\cos Q_{\rm MDM,E}\frac{v}{r_0}t-\hat{\mathbf{X}}\,\sin Q_{\rm MDM,E}\frac{v}{r_0}t\big), \tag{83}$$

where $(\hat{\mathbf{X}},\hat{\mathbf{Y}},\hat{\mathbf{Z}})$ is a triad of constant, orthogonal basis vectors in the particle rest frame. For circular motion in an electric field, $r_0E=\beta(pc/e)$, which leads to

$$Q_{\rm MDM,E}=G\beta^2\gamma-\frac{1}{\gamma}+1. \tag{84}$$

Accelerator spin physicists define the "spin tune" Q_s in an electric field by

$$Q_s\equiv\frac{d\alpha}{d\theta}\Big|_E=G\beta^2\gamma-\frac{1}{\gamma}, \tag{85}$$

where α is the angle between spin vector and particle velocity. The two definitions of "spin tune" have therefore been inconsistent. Unlike the beam direction, which advances by 2π each turn, and could therefore be described as having a "tune" value of 1, the spin tune is reckoned relative to the particle velocity rather than relative to a frame fixed in the laboratory. This accounts for the "+1" on the rhs of Eq. (84).) The content of this section has therefore amounted to being a derivation of Eq. (19), for the spin tune in an electric ring.

In the absence of betatron oscillations, Eq. (19), gives the dependence of spin tune on γ. In our (slightly) simplified model, the radial displacement x does not change on off-energy orbits, so there is no dependence on x in Eq. (19), hidden implicitly by longitudinal variation in γ around the ring.

"Spin tune" is a global invariant having much the same character as Ampère's law relating a line integral, $\int\mathbf{H}\cdot\mathbf{dl}$ to enclosed current; the line integral is unchanged by small alterations of the (closed) integration path. A non-vanishing betatron oscillation provides such a varied path, except that it is not closed. But such a betatron path, after a sufficient number of turns, will have returned to a point quite close to its starting point. Averaged over that duration, as a global invariant, the spin tune will be independent of horizontal betatron amplitude of any particular orbit.

Consider, then, the distribution function of all particles in the beam as a function of γ. Within a range $d\gamma$ this distribution will include orbits having all possible betatron amplitudes. By the previous paragraph, it will be legitimate regard Eq. (19) as being already adequately averaged over horizontal betatron oscillations—the only significant dependence is on γ.

B.3 EDM-Induced Precession in Electric Field

A particle at rest, with angular momentum $\mathbf{s}$ and electric dipole moment $d\,\mathbf{s}$, in electric field $\mathbf{E}'$, is subject to torque $d\,\mathbf{s}\times\mathbf{E}'$. Using Eq. (75), if the laboratory field is purely electric, the induced precession satisfies

$$\frac{d\mathbf{s}}{dt}\Big|_{\rm EDM,E} = d\,\mathbf{s}\times\mathbf{E}' = -d\,\mathbf{s}\times E\,\hat{\mathbf{x}}. \tag{86}$$

This precession is small enough to be treated as a perturbative addition to otherwise-inexorable polarization evolution.

To calculate EDM-induced precession we can use evolution formulas to describe dependence on θ, of the beam angle, which advances by 2π every turn. With $(\mathbf{X},\mathbf{Y},\mathbf{Z})$ being Cartesian coordinates fixed in the lab, setting $Q_{\rm MDM,E}=1$, as appropriate for frozen spin motion, the Frenet and spin vectors advance as

$$\begin{aligned}\hat{\mathbf{x}} &= \hat{\mathbf{X}}\,\cos\theta + \hat{\mathbf{Z}}\,\sin\theta,\\ \hat{\mathbf{s}} &= \hat{\mathbf{Y}}\cos\Theta + \big(\hat{\mathbf{Z}}\cos\theta - \hat{\mathbf{X}}\sin\theta\big)\sin\Theta.\end{aligned} \tag{87}$$

Here Θ is the polar angle of the polarization relative to the vertical axis. Substituting these on the right hand side of Eq. (86), the evolution of $\mathbf{s}_{\rm EDM,E}$ is the driven response given by

$$\begin{aligned}&\frac{v}{r_0}\,\frac{d\hat{\mathbf{s}}}{d\theta}\Big|_{\rm EDM,E} = \\ &\quad - d\,E\,\Big(\cos\Theta(-\hat{\mathbf{Z}}\cos\theta + \hat{\mathbf{X}}\sin\theta) + \sin\Theta\big(\cos\theta\big)\hat{\mathbf{Y}}\Big)\end{aligned} \tag{88}$$

References

[1] J.D. Jackson, *Classical Electrodynamics,* 3rd edition, John Wiley, 1999

[2] S.Y. Lee, *Spin Dynamics and Snakes in Synchrotrons* World Scientific, 1997